Chapter- 3

Tamarugite synthesis from white aluminium dross

Chapter 3

Tamarugite synthesis from white aluminium dross

3.1 Introduction to tamarugite

A natural mineral usually isolated from alum caves and volcanic sites around the world, tamarugite has a formula of $NaAl(SO_4)_2.6H_2O$ with monoclinic structure. Upon examination under SEM, plate-like morphology is observed. It is sodium aluminium sulphate hexahydrate, just like potash alum, but the number of water molecules associated to Tamarugite is 6. With a difference in the water of crystallization, Mendozite and Soda Alum are the double sulphate phases formed, number of water molecules being 11 and 12, respectively.

A few locations where tamarugite has been isolated from are Diana Caves at South West Romania, Wetlands around Blanchetown in Australia and Isle of Wight in the UK. This mineral has been studied in the field of Geology and its geological properties have been illustrated by many researchers [125]. The crystallographic data of this mineral are as follows [126]:

Tamarugite: Monoclinic $P2_1/a$, a = 7.3847 (3) Å, b = 25.2814 (15) Å and c = 6.1097 (3) Å, β = 94.85 (2) °

A few researchers have examined the thermal decomposition of tamarugite after isolation [125]. The samples had been obtained from southern Victoria, Australia and characterized using TGA.

This section illustrates the preparation, characterization and application of tamarugite. White aluminium dross powder has been utilized for the same. As explained in the previous chapter, the leaching of white aluminium dross is carried out to extract the

metallic values into the leach liquor. This liquor is then utilized for the preparation of tamarugite.

After the generation of synthetic tamarugite samples, the characterization has been described. The X-ray diffraction pattern and the SEM-EDS of the resultant product have been illustrated. The thermal decomposition of tamarugite has also been discussed. The characterization of the residual solid obtained after the thermal decomposition is also presented.

As tamarugite is a relatively rare mineral, the study of tamarugite as a coagulant explores the possibilities of its further application in this field. In this direction, the coagulation properties of tamarugite have been examined. Raw water samples from the Ganges (Assi Ghat, Varanasi) have been used for the tests. Some major conclusions from this study have also been discussed.

3.2 Synthesis and characterization of tamarugite

The aluminium content of tamarugite is leached from white aluminium dross. As described in the Chapter 2, the leaching of 4 g white aluminium dross powder is done using aqueous sodium hydroxide solution of 3 M concentration at 45 °C for 45 minutes. Sodium aluminate is produced when dross is leached with sodium hydroxide solution. Due to aluminium-water reaction, hydrogen is generated.

The addition of sulphuric acid (3 M) leads to the disintegration of $NaAl(OH)_4$ and formation of $Al(OH)_3$ and Na_2SO_4, as shown in the following equations (3.1-3.2) [127]. The aluminate reacts with the sulphate ions provided by the acid.

$$Al + H_2O + NaOH \rightarrow NaAl(OH)_4 + H_2 \quad (3.1)$$

$$2\ NaAl(OH)_4 + H_2SO_4 \rightarrow Na_2SO_4 + 2\ Al(OH)_3 + 2\ H_2O \quad (3.2)$$

As the first drop of sulphuric acid reacts with the leached filtrate, the generation of $Al(OH)_3$ takes place. A necessary step of processing is the stirring of the mixture with drop-wise addition of the acid using burette. This facilitates the formation aluminium sulphate with surplus acid added, as shown in eq. (3.3).

$$2\ Al(OH)_3 + 3\ H_2SO_4 \rightarrow Al_2(SO_4)_3 + 6\ H_2O \qquad (3.3)$$

Primarily, aluminium sulphate and sodium sulphate are generated in the solution mixture. Combined with essential molecules of water of crystallization, the crystallization of tamarugite takes place, as described in eq. (3.4).

$$Al_2(SO_4)_3 + Na_2SO_4 + 12\ H_2O \rightarrow 2\ NaAl(SO_4)_2.6H_2O \qquad (3.4)$$

The ionic equation for the formation of tamarugite can be written as eq. (3.5).

$$2\ Al^{3+} + 2\ Na^{+} + 4\ SO_4^{2-} + 12\ H_2O \rightarrow 2\ NaAl(SO_4)_2.6H_2O \qquad (3.5)$$

Thus, a process with sequential steps involving chemical reactions leads to the crystallization of tamarugite. It has been found that the formation of tamarugite is exothermic and the enthalpy of formation $\Delta H°_{f298.15K}$ of Tamarugite at room temperature (298.15 K) is nearly – 4271.15 ± 26 kJ/ mol [128].

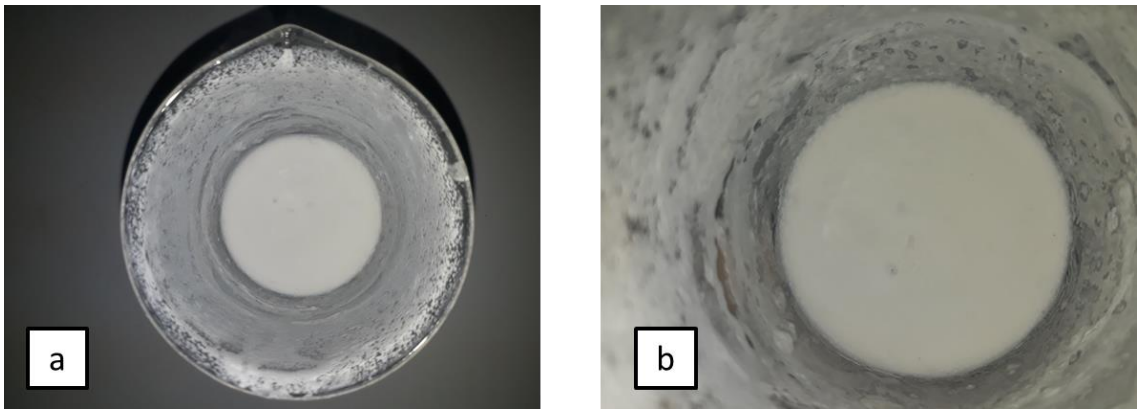

Figure 3.1.a. Photographic image of the formation of tamarugite from the saturated solution prepared, 3.1.b. a magnified image of the beaker with tamarugite

It can be seen from figure 3.1 that the Tamarugite has precipitated onto the walls of the beaker. A photographic image showing the top view of the beaker (Figure 3.1.a) simply illustrates this fact. A magnified image on the right (Figure 3.1.b) shows that the contact of the saturated solution with the walls of the beaker has given plenty of nucleation sites from which Tamarugite particles have successfully grown.

It should be noted here that most of the saturated solution was at the bottom of the beaker and only a small fraction of the liquid came in the contact of the walls. Therefore, the thickness of the tamarugite crop is quite higher at the bottom of the beaker and relatively less at the beaker walls. The precipitated tamarugite has been scrapped out of the beaker after its complete solidification and subjected to further characterization using XRD, SEM-EDS and TGA facilities.

During the initial trials of crystallization of tamarugite, glass beakers had been used. It turned out that the crystallized tamarugite was very difficult to isolate from the beaker, as the crystallized tamarugite was very hard. Further experiments of crystallization of

tamarugite have been done using plastic beakers for the ease of separation of the resultant crop.

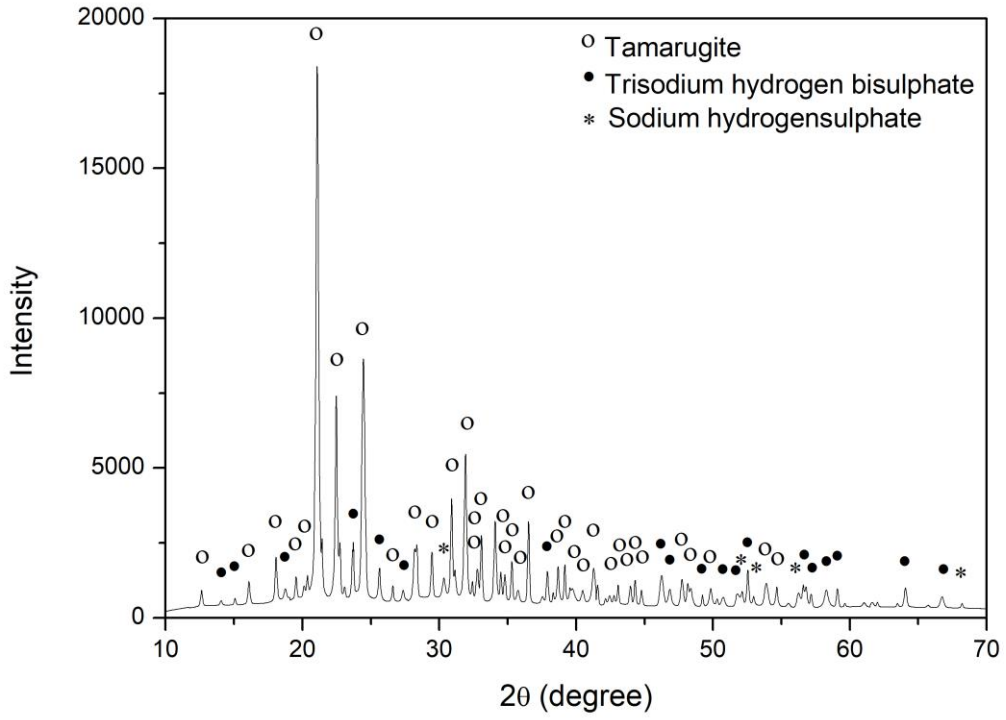

Figure 3.2: X-ray diffraction pattern of tamarugite

The XRD pattern for tamarugite has been obtained (Figure 3.2) for a 2θ range of 10° to 80°. The major peaks of tamarugite are at 21.08°, 22.50°, 24.50° and 31.98°. Analysis the XRD pattern of the precipitated product shows that the major phase present in the solid product is tamarugite, $NaAl(SO_4)_2.6H_2O$ and the minor phases are trisodium hydrogen bisulphate, $Na_3H(SO_4)_2$ (PCPDF file no: 01-077-4541) and sodium hydrogen sulphate, $NaHSO_4$ (PCPDF file no: 01-077-4541).

Since aluminium is not present in the side products, aluminium must have been transferred from aluminium dross to sodium aluminate and then further into tamarugite. The complete solution mixture precipitated to provide the resultant product. No residual

liquid was left behind. In other words, all the amount of aluminium present in the solution must have ended up into the tamarugite phase. The other reaction species present in the solution mixture include sodium and sulphate ions. The presence of these free ions must lead to the formation of these other phases.

In order to understand the transfer of aluminium from white aluminium dross to the resultant tamarugite, the complexometric titrations of the leach liquor have been carried out. As mentioned above, no residual liquor was left after the tamarugite crystallization. This implies that aluminium leached into the liquor was transformed into tamarugite.

For this analysis, the leaching experiment had been replicated with the parameters described before. The complexometric titrations using disodium salt of EDTA and EBT as indicator were done. To confirm the amount of aluminium present in the solution, the titrations and the leaching experiment has been repeated twice and the average amount has been calculated. It has been found that nearly 2.26 g of aluminium had successfully leached into the solution. Since aluminium partitioning is not observed, the complete amount was used to generate tamarugite crop.

Figure 3.3 shows the scanning electron micrographs of tamarugite. At lower magnifications, random particles appear and these large agglomerates of particles are of around 100 μm size. As the magnification is increased, the particles of tamarugite are more clearly visible and the plate-like morphology is observed.

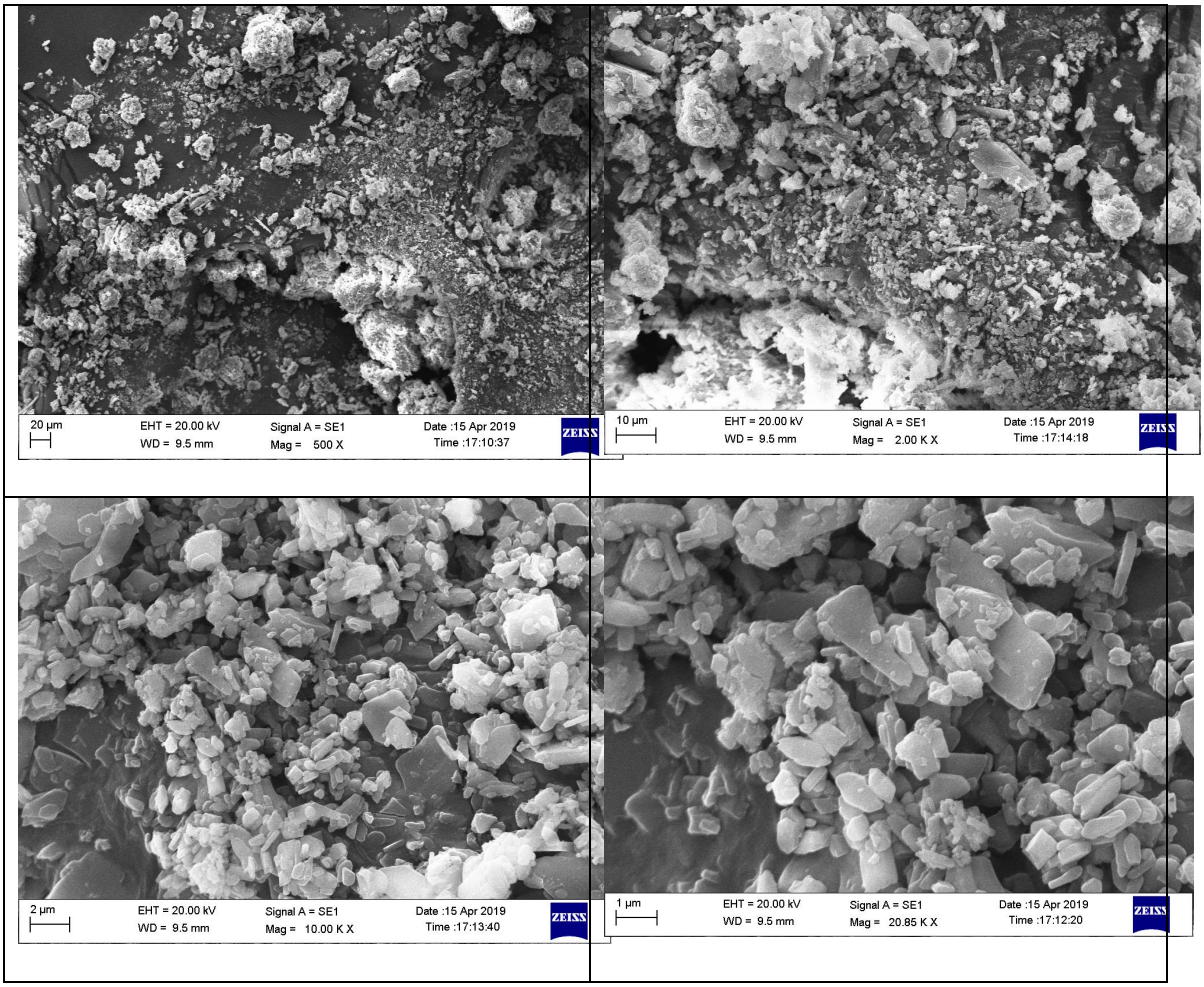

Figure 3.3: Scanning electron micrographs of tamarugite at 500x, 2000x, 10000x, and 20850x

At even higher magnifications, the random arrangements of plates are observed. Further examination of the sample at higher magnifications suggest that the structure has potash alum-like plates, however these plates are irregularly oriented and the size of these planar structures is variable. Some of these plates are parallel, whereas others are perpendicular to the planes. On the corners of the micrograph, small planer structures are also visible. These structures also show the formation of small plates in random fashion.

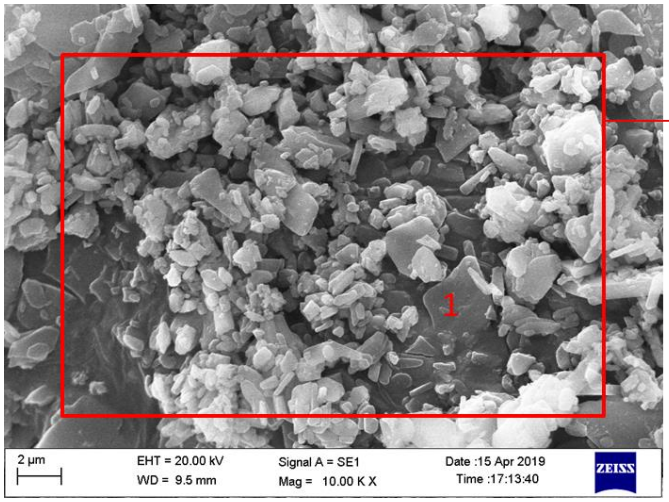

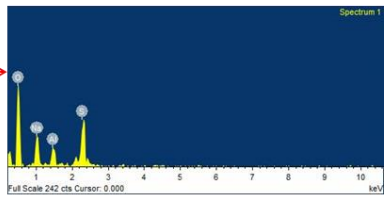

Element	Weight %	Atomic %
O K	64.84	75.61
Na K	14.25	11.57
Al K	5.96	4.12
S K	14.95	8.70

Point 1

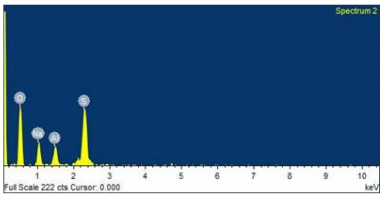

Element	Weight %	Atomic %
O K	63.16	74.99
Na K	10.91	9.02
Al K	5.71	4.02
S K	20.21	11.97

Figure 3.4: SEM-EDS of tamarugite produced from white aluminium dross

As observed from figure 3.4, the elements identified are sodium, aluminium, sulphur and oxygen. Sulphur varies from 14.9 to 20.2 wt. % and oxygen is around 63.1 to 64.8 wt. %. Sodium and aluminium are present in the sample and the amount of sodium is in greater quantity than aluminium. The point spectrum shows nearly 5.7 wt. % aluminium, compared to 10.9 wt. % sodium, whereas the area spectrum around 5.9 wt. % aluminium and 14.2 wt. % sodium.

This fact also supports the slight domination of sodium's quantity in the precipitated product. The minor phases detected in the XRD are sulphates of sodium. Therefore it is fair to understand that the higher amount of sodium may have led to the precipitation of sodium sulphate products.

To further study the composition of tamarugite, ICP-OES analysis has been done. Aqueous solutions of tamarugite have been prepared and diluted. The dilution has been done such that the amounts of aluminium and sodium present in the solution are within the detection limit of the instrument (in the range of parts per million). It has been found that 1.148 mg/L sodium and 0.480 mg/L aluminium are detected.

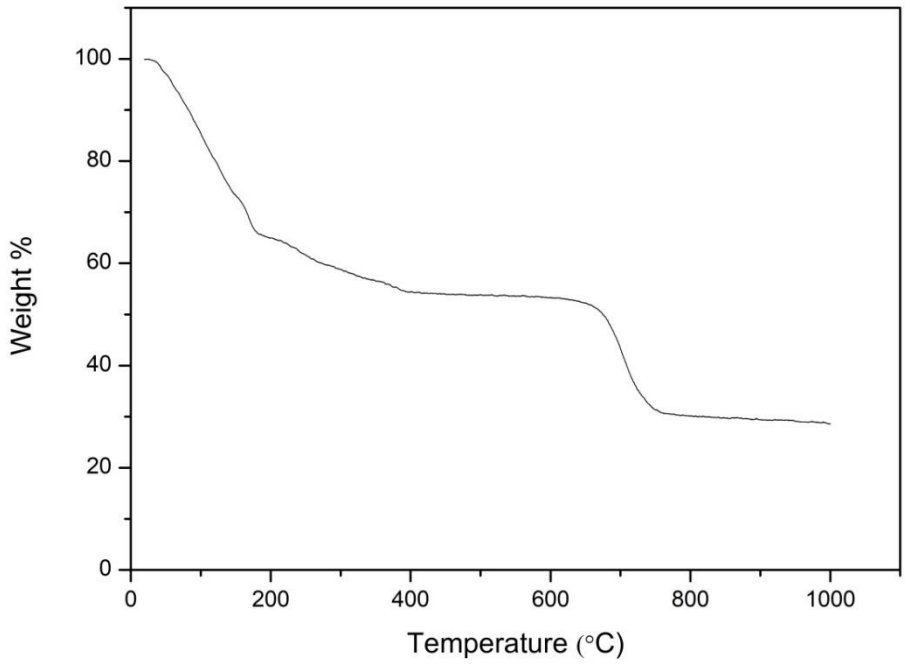

Figure 3.5 TGA of tamarugite produced from white aluminium dross

Figure 3.5 illustrates the Thermogravimetric Analysis of the synthetic tamarugite. As can be understood by observing the TGA plot, the crystallized tamarugite sample undergoes two major mass loss zones (between 30 – 400 °C and 650 – 800 °C). The TGA plot has been fitted linearly using Origin software (version 8.0724) to determine the transition temperatures within the plot to understand the mass loss relation with respect to temperature change. The transition temperatures observed from the analysis are 182 °C, 389 °C and 670 °C and 740 °C for the two temperature ranges.

The first mass loss observed in the temperature range of 30 – 400 °C is explained with the loss of water of crystallization. This has been confirmed by the calculation of the mass loss and comparing it with the stoichiometry of tamarugite. It has been found that number of molecules associated with tamarugite is 6, as governed by its chemical formula, $NaAl(SO_4)_2.6H_2O$ [125]. This has been determined by determining the actual mass loss and stoichiometric calculations.

After this temperature range, the other major mass loss is observed in 650 – 800 °C. As described by various other researchers, the major mass loss in this region may be due to the release of SO_3 gas and the decomposition of aluminium sulphate [125, 129, 130]. Since this transition takes place simultaneously, it can be seen that drop in this region is very smooth.

As described in literature, the weight loss curves are associated to the loss of water molecules and the release of sulphur trioxide gas [125]. A range of phases have been reported to be present at the end of the examination. After the loss of SO_3 gas, $Na_2SO_4.Al_2(SO_4)_3$ and other unidentified phases have been reported, whereas in other research, the formation of aluminium oxide takes place.

After the TG analysis of tamarugite, the resultant solid has been subjected to XRD analysis to determine the phases present in it. The major phases present in it are aluminium trioxide and disodium sulphate. Therefore, it is seen that the SO_3 gas released was due to the decomposition of aluminium sulphate, whereas sodium sulphate remained pristine. The XRD pattern of the residual tamarugite has been shown in figure 3.6.

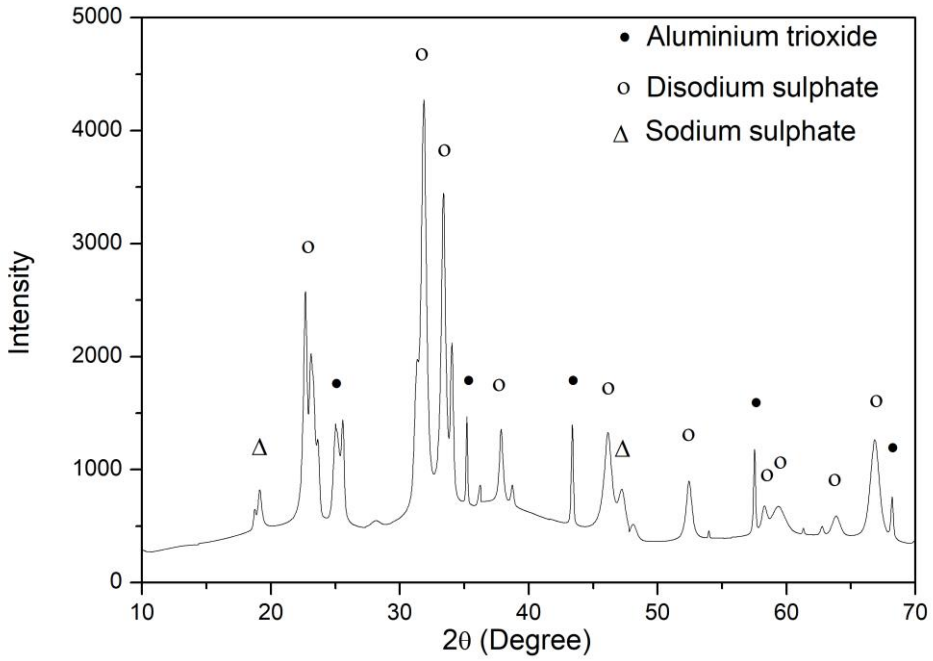

Figure 3.6: XRD pattern of residual solid of tamarugite obtained after heating it at 1000 °C

3.3 Applications of tamarugite: Coagulation

As mentioned previously, tamarugite has not been explored completely and a lot needs to be studied about it. The application of tamarugite is one segment where the present work has been carried out. Tamarugite dissolves quickly in water. This suggested that the mineral supplied Na^{+}, Al^{3+} and SO_4^{2-} ions simultaneously to the water. Looking at the chemical formula of tamarugite, it is seen that it is sodium aluminium sulphate hexahydrate.

Aluminium sulphate has coagulating properties. It is also known as the papermakers' alum. The coagulation tendency of aluminium sulphate comes from the aluminium ions. The phenomenon of coagulation is described later in this section. If aluminium sulphate could be used as a coagulant, the same could be done for tamarugite as well.

To verify this, a preliminary test of coagulation has been conducted using tamarugite as a coagulant. A colloid has been prepared using distilled water and dried soil. 100 mL of this colloidal solution was equally partitioned in two 100 mL beakers; in one of the beakers nearly 0.3 g of tamarugite was added. It has been observed that within 5 minutes of tamarugite addition, the turbidity of the colloidal solution decreased. The solid particles had settled at the bottom of the beaker and clear water was obtained at the top of the beaker. The photograph of the same is shown in the figure 3.7.

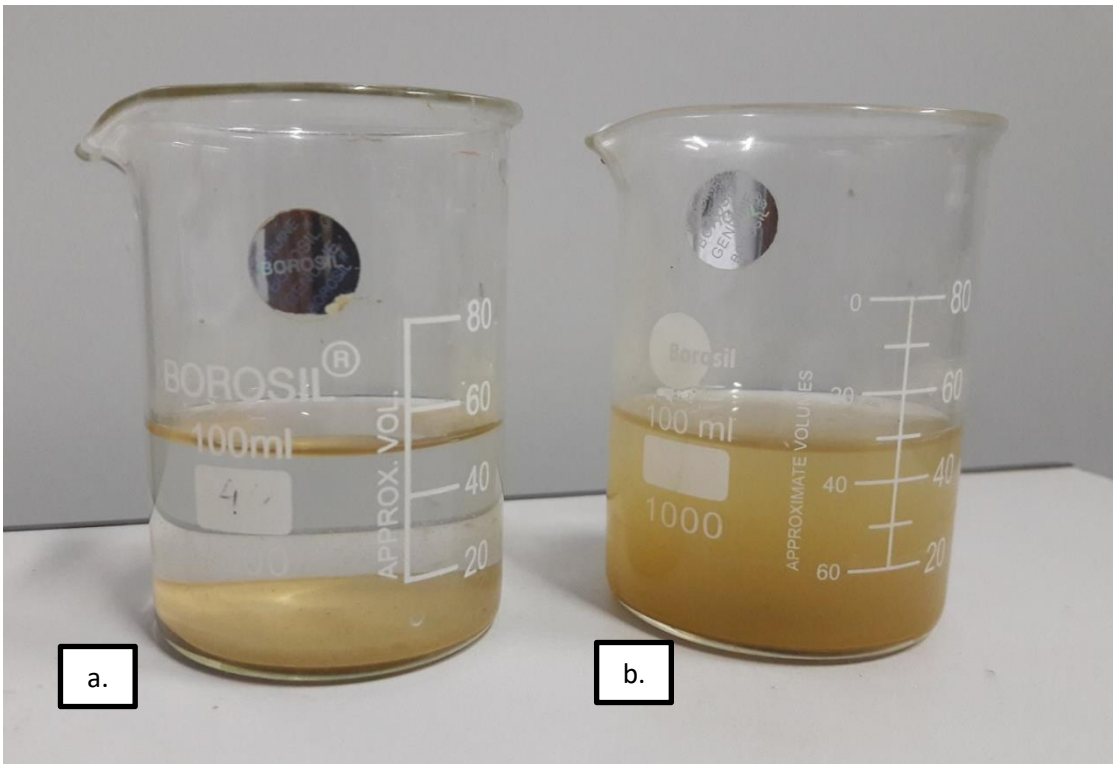

Figure 3.7: Effect of tamarugite addition on coagulation: a. with addition of tamarugite and b. without tamarugite

From the figure, it is observed that the colloidal particles settled due to the coagulating tendency of tamarugite. In contrast to the coagulation, the water in the other beaker remains turbid. The colloidal particles are stable here. There is no sign of self-agglomeration and settling of the colloidal particles present in the water sample. This

test, however, merely confirms the tendency of tamarugite. A proper quantitative analysis of the coagulation property was necessary.

3.4 Coagulation of colloidal particles: Jar Test

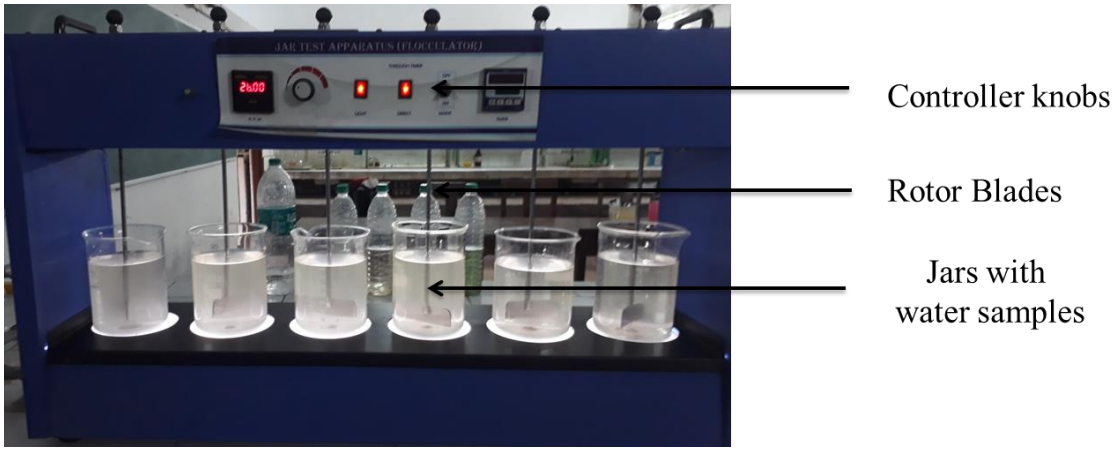

Figure 3.8: Jar Test conducted with tamarugite as coagulant

After the confirmation of the coagulation property of synthetic tamarugite, the quantitative study of the coagulation has been done. For this, the standard Jar test has been done, where the raw water samples have been used. The Flocculator apparatus has been employed for this test. As described in the Chapter 2, the raw water samples have been collected from the *River Ganga at Assi Ghat, Varanasi*. For every test a water container of 5 L capacity was refilled. The turbidity of the raw water samples was measured before and after the test for every jar and it was ensured that the jars contained water with similar turbidity values.

When the turbidity of the raw water samples varied in a very large range, the water samples were allowed to settle at the jars for a few minutes. This led to the settling of larger particles at the bottom of the jars, the colloids present in the water samples still remained suspended. The turbidity of the water samples comes from these colloidal

particles that are stable in water. It is these particles that need to be settled to remove the turbidity.

As shown in figure 3.8, in a single turn of the Jar Test, six samples of raw water are characterized. Filled with raw water, 1 L beakers are placed at the Flocculator apparatus. The initial turbidity is determined to ensure similar turbidity for every jar. This is done by drawing around 10 mL of raw water sample from around the middle of the jar and introducing it to the small bottle used for the turbidity measurement. This bottle is handled with due care, such that no scratches appear on its exterior. It is wiped with a tissue paper to ensure the bottle's dryness. This bottle is then placed into the sample chamber of the Nephelometer. The Nephalometer is the device used to measure the turbidity of the water samples; it measures the turbidity in NTU (Nephelo Turbidity Unit). It is necessary to calibrate the instrument before its use for accurate results (Figure 3.9). After measuring the turbidity of raw water samples, the rotor blades are inserted into the jars.

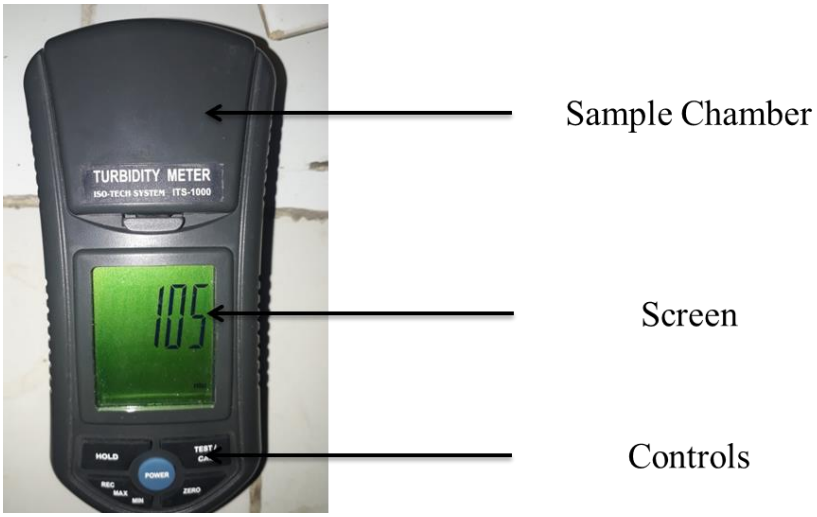

Figure 3.9: Nephelometer used for measuring turbidity of water samples

The coagulant solution is prepared of tamarugite of a concentration of 1 g/L and a varying dosage of coagulant solution is added to each jar. This is done to study the effect of coagulant dose on the turbidity of the raw water samples. The coagulant dosage provided into the water samples disturbs the charge cloud around the colloidal particles and this causes the coagulation of the particles. The acceptable value of turbidity in water samples is less than 5 NTU in India. The objective of the study is to reduce the turbidity of the raw water samples to a value as low as possible. Increasing the dosage of the coagulant solution leads to the rise in the turbidity of the water sample. The charge reversal of the colloidal particles is the major reason behind this phenomenon, further leading to the stabilization of the particles in the water.

After the addition of dosage of coagulant solution of tamarugite is done, the blades are rotated for a period of 120 seconds at 100 rpm. This is the period of the test when the coagulant comes in the contact with the stable colloids and interacts with them. At the end of the period, the rotation of the blades is reduced to around 20 rpm and maintained for nearly 20 minutes. During this period, the formation of the flocs can be observed in the jars. These flocs tend to agglomerate and move around with the rotation of the blade. At the end of this slow agitation period, large flocs of colloidal particles are clearly visible. The rotation of the blades is stopped and the raw water samples are left undisturbed for another 20 minutes.

Due to the presence of the colloidal particles, the raw water appears cloudy during the flocculation stage. These colloidal particles move in the rotation, following the rotation of the blade. During the settling stage of the test, the flocs of the colloidal particles are larger and settle down at the centre of the jars due to the gravity. This settling tendency has been observed in the jar tests.

Figure 3.10 vividly illustrates the settling of the colloidal particles after the jars are left undisturbed in the Flocculator. The raw water samples obtained after the Jar Test are clearly less turbid and show significant drop in the turbidity. The final turbidity of the raw water sample is measured such that the bottom layer of the settled flocs of colloidal particles is not disturbed. For this, a pipette is inserted into the raw water jar and carefully samples are collected. These water samples are subjected to turbidity testing using Nephalometer mentioned above.

As explained later in the next sections, the addition of the coagulant solution to the raw water leads to the disturbance of charge cloud around the colloidal particles. This further leads to the capture and entrapment of colloidal particles into the gelatinous and amorphous aluminium hydroxide. The colloidal particles have settled and formed a pile at the bottom of the beaker and the water now appears to be free from turbidity. The mechanism of the coagulation has been discussed in the next section.

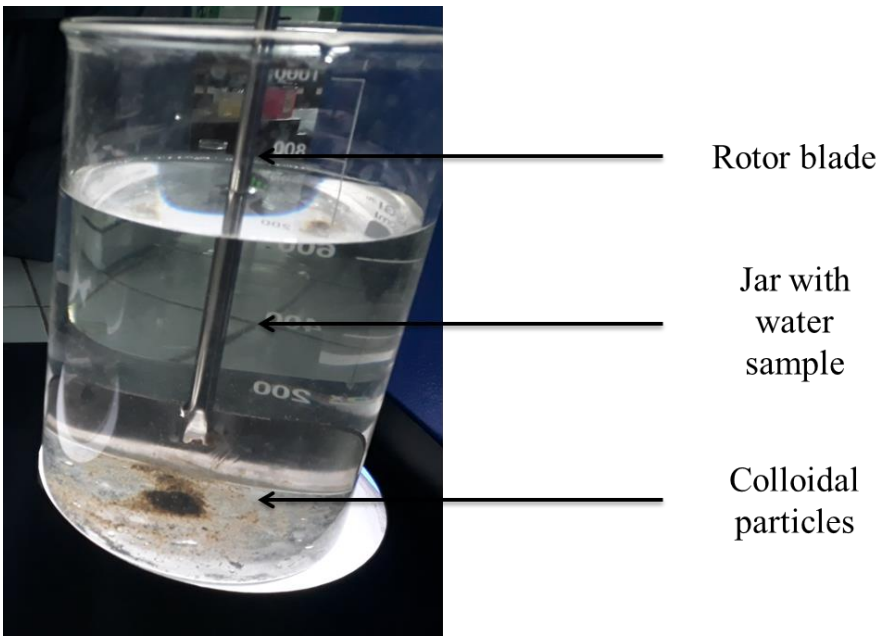

Figure 3.10: A Jar with raw water showing the settled colloidal particles

The coagulation of the colloidal particles is clearly seen in the above photograph. The particles tend to move in a random Brownian motion and after the standard procedure of rotation of the water sample is stopped, the particles collide with each other to settle down. The brown residue at the bottom of the jar is the agglomeration of the colloidal particles initially present in the raw water sample.

3.5 Mechanism of coagulation

It is essential to grasp the nature of the colloidal particles prior to appreciate the mechanism of coagulation upon the addition of tamarugite. Due to the accumulation of the charge around the some colloidal suspensions, the natural settlement of these particles is hindered. These suspensions are referred to as stables [131]. The larger particles present in the raw water tend to settle down on their own, due to their larger mass and gravity. As mentioned in above, it is the smaller, stable colloidal particles that are the main contributors to the turbidity of the water. In most of the cases, the charge accumulated around these stable colloidal particles is negative.

When coagulant dose is provided to the raw water, it interacts with the negatively charged colloidal particles and disturbs the charge cloud around it. It is essential to overcome the energy barrier of the two opposing forces to initiate the coagulation process. The two forces are the Zeta potential of the particles and the van der Waals force.

A negatively charged colloidal particle has a positive charge accumulation around it. This is because the negative charge of the particle shall attract the positive charge around it. When many such negatively charged particles are present in the water, there is repulsion between the particles. This is due to the repulsion of the positive charge around the negatively charged colloidal particles. This repulsive force is called Zeta

potential. On the other hand, there is the van der Waals force that causes the attraction of the colloidal particles to each other.

It is the coagulant introduced into the water that surpasses the energy barrier and brings the particles close enough to be agglomerated and settled. To form the microflocs and subsequently the microflocs, the charge neutralization of the particles is necessary. This is done by the addition of coagulant to the water samples. Van der Waals forces overcome the Zeta potential to form the flocs. Addition of polymers can be required to keep the flocs together.

Usually, the salts of Al^{3+} and Fe^{3+} are used for the coagulation because these salts dissociate into complex products, which are aquometallic in nature. Examples of these complex are $Al(H_2O)_6^{3+}$ and $Fe(H_2O)_6^{3+}$. These complex products undergo hydrolysis reactions, where the H_2O molecules are replaced by OH^- ions to form $Al(OH)^{2+}$ and $Fe(OH)^{2+}$, as shown in the eq. (3.6-3.9). These reaction products are highly efficient in coagulant the negatively charged colloidal particles.

$$\{Al(OH_2)_6\}^{3+} \rightarrow \{Al(OH)(OH_2)_5\}^{2+} + H^+ \quad (3.6)$$

$$2\ \{Al(OH_2)_6\}^{3+} \rightarrow 2\ \{Al(OH)(OH_2)_5\}^{2+} + 2\ H^+ \quad (3.7)$$

$$17\ \{Al(OH_2)_6\}^{3+} \rightarrow 17\ \{Al(OH)(OH_2)_5\}^{2+} + 17\ H^+ \quad (3.8)$$

$$Al^{3+} + 3\ H_2O \rightarrow Al(OH)_3 + 3\ H^+ \quad (3.9)$$

The final stable compound formed is aluminium hydroxide, $Al(OH)_3$. Also, a hypothetical neutral charged specie $\{Al(OH)_3(OH)_6\}^0$ (point zero charge) is produced. These compounds condense with each other resulting in essentially amorphous and gelatinous mass. The compound formed helps in the accumulation and the settlement of the colloidal particles. The entrapment of the colloidal particles is one of the methods.

The other is the enmeshing of the particles with the hydroxide, due to the sticky nature of the hydroxide [135].

The particles are also swept with the amorphous aluminium hydroxide, which leads to the settling of the particles. Thus the coagulation of the particles takes place. The coagulation effect of tamarugite on the turbidity of the water samples is seen in Figure 3.11.

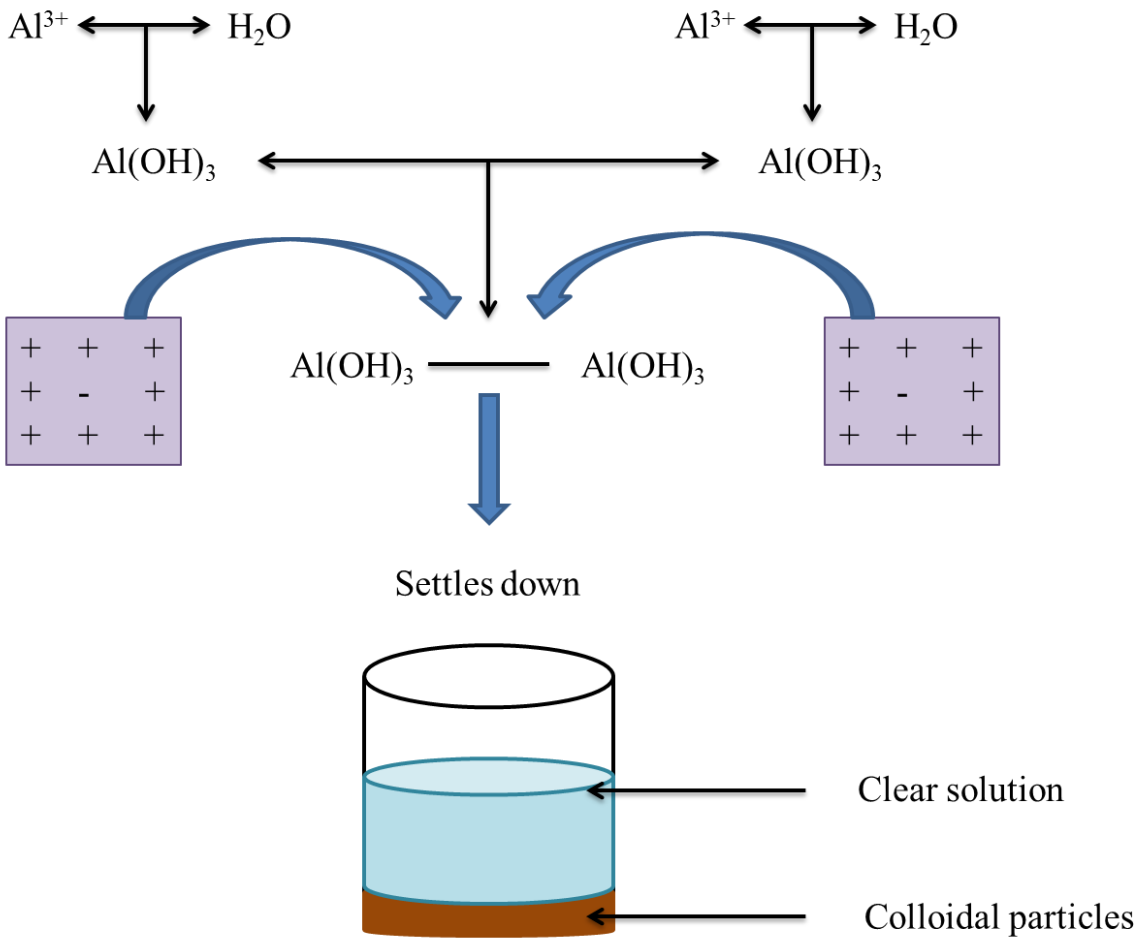

Figure 3.11: Mechanism of coagulation with the addition of coagulant

The figure illustrates the formation of $Al(OH)_3$, agglomeration of the hydroxide particles, and gathering the colloidal particles, either by entrapping them or enmeshing them. This is done within the initial stages of the jar test, when coagulant is added. The

formation of microflocs follows; the flocs grow in size and mass, leading to the settling of the particles at the bottom. This marks the completion of the coagulation process. The water treatment plants work on the same principle, although the addition of coagulant is optimized continuously to maintain the process. The amount of the coagulant added depends on many factors; the initial turbidity and pH of the water are very important parameters for coagulation.

3.6 Coagulation test results

As mentioned previously, the turbidity values have been determined before and after the coagulation test. The fractional change in turbidity has been reported in the results, denoted by Δt. This is the change in turbidity with respect to the initial turbidity. With increase in the dosage of the coagulant solution, the coagulation also increases, as shown in Table 3.1. The coagulation experiments have been repeated with commercial alum for proper comparison.

Table 3.1: The variation of aqueous tamarugite solution with the turbidity and pH of the water samples in Jar Test

Sample Number	Coagulant Concentration in mg/L	pH of Raw water		Fractional Change in Turbidity of Raw water	
		Commercial Alum	Tamarugite	Commercial Alum	Tamarugite
1.	Nil	7.53	7.53	0	0
2.	2	7.65	7.2	0.73	0.70
3.	4	7.55	7.1	0.81	0.80
4.	6	7.48	7.1	0.89	0.86
5.	8	7.35	7.16	0.94	0.90
6.	10	7.4	7.11	0.96	0.93
7.	12	7.35	7.1	0.97	0.96

The fractional change in the turbidity of the solution is increased; this is clearly due to the increased action of the coagulant added to the water samples. With just 2 mg/L of

the coagulant dosage for both alum and tamarugite, a sharp change in the value of Δt is observed. From control value, Δt rose to 0.7 in both the coagulants.

With the increase in the dosage of the coagulants, the values of Δt reach a saturation point at nearly 12 mg/L. Here the fractional turbidity approaches unity. With greater dosage of coagulant, the final turbidity also increases and therefore, the value of Δt drops again. This is due to the charge reversal of the colloidal particles. Excessive addition of the coagulant leads to the stabilization of the charge of the particles, thereby increasing the turbidity.

Apart from the values of Δt, the changes in pH of the water samples have also been noted. For both the coagulants, the pH remained within the range of 6-8. The drop in pH for tamarugite is greater (from 7.53 to 7.10), compared to the commercial alum (7.53 to 7.35). The drop in the pH of the water samples is not very sharp and this is an advantage for tamarugite. Any sharp change in pH of the water leads to another step of pH maintenance.

The fractional change in the turbidity due to the addition of the coagulant is shown in Figure 3.12. At nearly 12 mg/L, the both the coagulants have almost the same values of Δt. As a trend, it is true that commercial alum is a better coagulant, but tamarugite has been consistently performing well and competes with commercial alum.

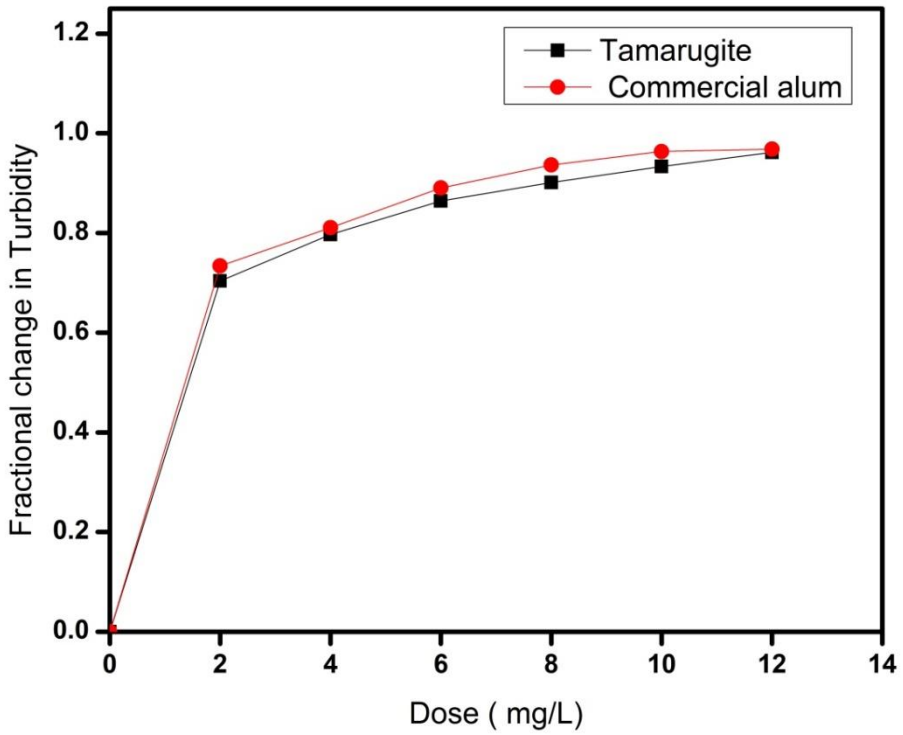

Figure 3.12: Fractional change in turbidity of raw water with the variation of coagulant dose

The major reason behind the lack of coagulation is due to the presence of the other phases in the tamarugite resultant product. It has been suspected that if the purity of tamarugite is increased by some means, the coagulation performance of the solution will also increase. The next section describes the synthesis of Tamarugite using organic solvent precipitation. The presence of other phases is reduced by a large margin, providing a purer tamarugite phase. The Jar Test of the said sample is described therein. Results are quite encouraging.

In general, it can be deduced that tamarugite is a good material for coagulation applications. The colloidal particles present in the wastewater can be easily settled and removed to provide clear and turbidity-free water. Competing with the commercial

alums used for the coagulation applications, it is believed that tamarugite may be a potential coagulant for industrial utilization with further studies.

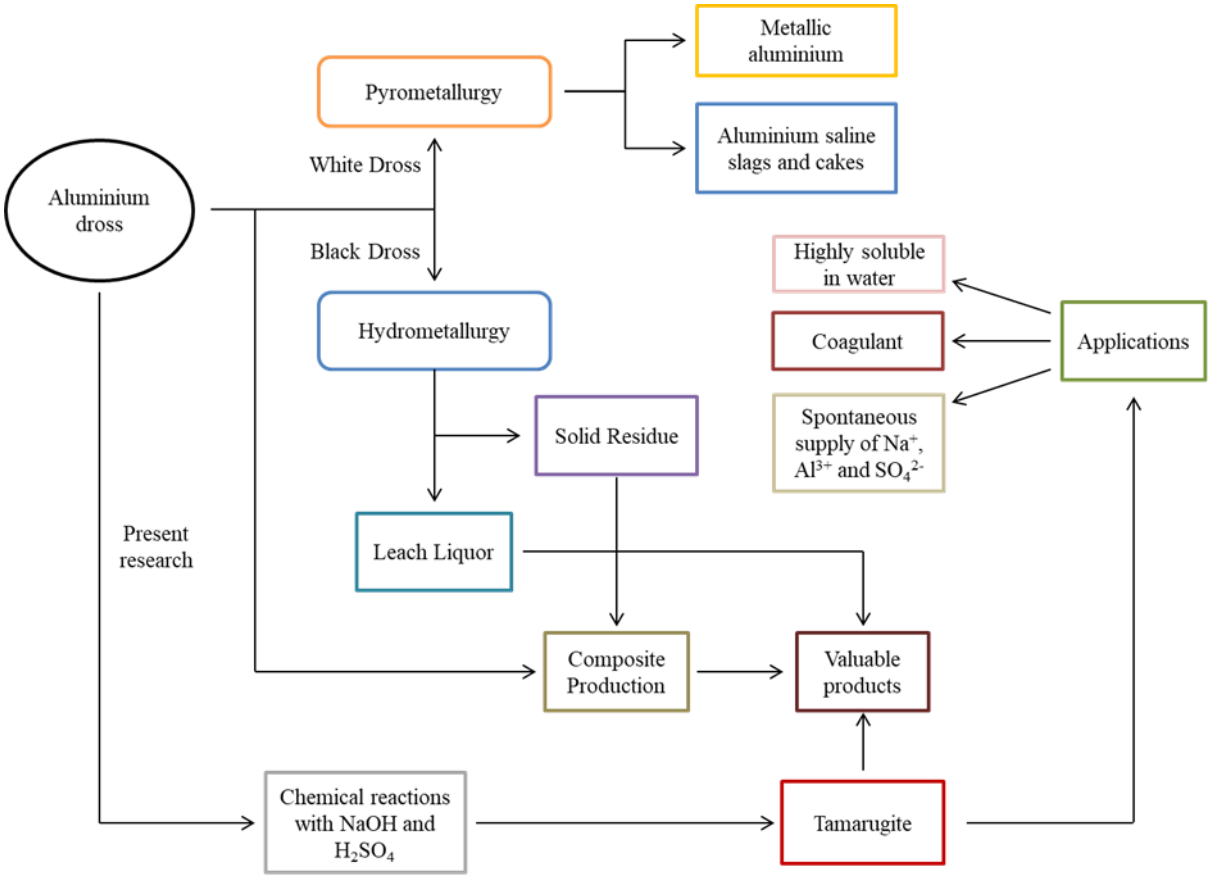

Figure 3.13: Flow sheet illustrating the conventional routes of recycling aluminium dross with synthesis of tamarugite

As can be observed from figure 3.13, aluminium dross is employed for a whole variety of processes to produce a plethora of important products. A generalized notion can be developed after studying the present flow sheet. The conventional method of recycling white aluminium dross is to subject it to pyrometallurgical operations, extracting metallic aluminium from it, leaving behind aluminium saline slags and salt cakes. When salt free technologies are used for the metal extraction, the non-metallic product with very less aluminium content is left over after the dross processing.

If aluminium dross is having lower amount of metallic aluminium (usually black aluminium dross), it is subjected to hydrometallurgical operations, where it is leached using various media (acidic or alkaline) and metallic content present in the dross is extracted into the aqueous solutions. These aqueous solutions are utilized to produce various important industrial products. The residual solid obtained after the metal extraction from hydrometallurgical solid still has some amount of aluminium. It may also contain other phases that were unaffected by the leaching media. This solid residue can be used to produce composites.

The residual solids have been utilized as reinforcements for composites, as additions to the matrix phase. Al-Al_2O_3 composites have been well explored and studied. The residual solid can be used to produce Al_2O_3 and then consumed for the composite production. The use of aluminium dross as a reinforcement has also been described in the literature. Other types of composites like mullite-zirconia composites are prepared by directly using aluminium dross.

Lastly, the present work is shown where white aluminium dross is utilized for the crystallization of tamarugite. It can be synthesized by chemically reacting it with NaOH and H_2SO_4. Some of the potential applications can be in the field where aluminium, sodium and sulphate ions simultaneously required. The dissolution of tamarugite is quick and as described above, it has good coagulation properties.

3.7 Conclusion

This section broadly describes the synthesis of tamarugite, a relatively rare mineral, using aluminium dross as a raw material. The powdered white aluminium dross has been reacted with aqueous sodium hydroxide solution to produce sodium aluminate in the aqueous solution. This solution is subjected to reaction with sulphuric acid solution.

Aluminum hydroxide tends to form in the solution with the first drop of sulphuric acid. After complete addition of the required amount of sulphuric acid solution into the leached sodium aluminate solution, the solution mixture is heated to achieve saturation. This solution simply produces tamarugite as it cools to the room temperature. This product has been characterized and it has been found that the major phase comprises of tamarugite, other phases being trisodium hydrogen bisulphate $Na_3H(SO_4)_2$ and sodium hydrogen sulphate $NaHSO_4$.

Observing the scanning electron micrographs of the synthetic tamarugite, it has been deduced that the plate like structure seen in the micrographs are quite similar to the plate like structures seen in the natural mineral isolated from its natural habitats. The TGA of the synthetic tamarugite shows that the first major drop in weight is due to the loss of water of crystallization whereas the second drop is due to the dissociation of aluminium sulphate and conversion into alumina, accompanied with the release of SO_3 gas. The phases present in the solid residue are aluminium trioxide and disodium sulphate.

Even after synthesizing tamarugite from white aluminium dross, the application of the product came as a challenge. This necessitates a greater study of tamarugite's properties and its application in various fields. The notion of using tamarugite for the coagulation came from the fact that aluminium sulphates can be used as coagulants as these tend to form aluminium ions in the water. If regular aluminium sulphate can be subjected to coagulation, the same can be done with tamarugite, which just a double sulphate salt. With the idea of using tamarugite as a coagulant to treat wastewater samples, Jar test has been carried out to study its coagulation properties.

When Tamarugite is subjected to Jar Test to coagulate the colloidal particles present in the wastewater, it functions on par with the commercial alum used for the purpose of the coagulation. The colloidal particles get entrapped along with the aluminium hydroxide produced when tamarugite solution is added to the wastewater samples. Finally the colloidal particles settle down at the bottom of the beaker, clearing the water.

To conclude this section, it is essential to understand that a waste industrial by-product has been successfully recycled to produce a relatively rare mineral, which has further been utilized as a coagulant to settle the colloidal particles in wastewater. Being a rare mineral, properties and applications of tamarugite have not been studied thoroughly. In the present work, tamarugite is studied as a coagulant, which can be confirmed from the results of the Jar Test.

The synthesis of tamarugite is a method of recycling white aluminium dross by using simple chemicals and following simple reactions. It is vital to look at the big picture while understanding this process of recycling aluminium dross. The holistic view illustrates the waste management of aluminium dross, its step-by-step recycling and production of tamarugite, a valuable product and its utilization of waste water treatment. As tamarugite finds its application in coagulation, a new horizon of research is opened.

In the next chapter, aluminium dross is used to synthesize tamarugite using organic solvent precipitation. The method described therein is an alternative method of producing tamarugite.